DESY 01–130
TTP01–21
hep-ph/0109084
September 2001

Determination of α_s and heavy quark masses from recent measurements of $R(s)$

J.H. Kühn[a] and M. Steinhauser[b]

(a) Institut für Theoretische Teilchenphysik,
Universität Karlsruhe, D-76128 Karlsruhe, Germany

(b) II. Institut für Theoretische Physik,
Universität Hamburg, D-22761 Hamburg, Germany

Abstract

In this paper we compare recent experimental data for the total cross section $\sigma(e^+e^- \to \text{hadrons})$ with the up-to-date theoretical prediction of perturbative QCD for those energies where perturbation theory is reliable. The excellent agreement suggests the determination of the strong coupling α_s from the measurements in the continuum. The precise data from the charm threshold region, when combined with the recent evaluation of moments with three loop accuracy, lead to a direct determination of the short distance $\overline{\rm MS}$ charm quark mass. Our result for the strong coupling constant $\alpha_s^{(4)}(5\text{ GeV}) = 0.235^{+0.047}_{-0.047}$ corresponds to $\alpha_s^{(5)}(M_Z) = 0.124^{+0.011}_{-0.014}$, for the charmed quark mass we find $m_c(m_c) = 1.304(27)$. Applying the same approach to the bottom quark we obtain $m_b(m_b) = 4.191(51)$ GeV. Whereas our result for $\alpha_s(M_Z)$ serves as a useful cross check for other more precise determinations, our values for the charm and bottom quark masses are more accurate than other recent analyses.
PACS numbers: 12.38.-t 14.65.Dw 14.65.Fy

1 Introduction

The strong coupling constant and the quark masses are the basic input parameters for the theory of strong interaction. Quark masses are an essential input for the evaluation of weak decay rates of heavy mesons and for quarkonium spectroscopy. The prediction of these masses is an important task for all variants of Grand Unified Theories. To obtain the values in a consistent way from different experimental investigations is thus a must for current phenomenology.

During the past years new and more precise data for $\sigma(e^+e^- \to \text{hadrons})$ have become available in the low energy region between 2 and 10 GeV. At the same time increasingly precise calculations have been performed in the framework of perturbative QCD (pQCD), both for the cross section as a function of the center-of-mass energy $\sqrt{s}$, including quark mass effects, and for its moments which allow for a precise determination of the quark mass. A fresh look at the determination of the strong coupling and the quark masses based on these new developments is thus appropriate.

For the determination of α_s we shall use energy regions sufficiently far away from the threshold where pQCD plus local duality is expected to give reliable predictions. For the determination of the quark masses we will use sum rules where the input depends heavily on the threshold region with its rapidly varying cross section.

Sum rules as tool to determine the charm quark mass have been suggested by the ITEP group long ago [1]. Subsequently these methods have been developed further [2] and frequently applied to the bottom quark. Most of these later analyses concentrated on using relatively high moments which are less sensitive to the continuum contribution and exhibit a very strong quark mass dependence. However, this approach requires the proper treatment of the threshold, in part the resummation of the higher order terms of the Coulombic binding and a definition of the quark mass adopted to this situation like the potential- or $1S$-mass [3, 4]. Recently improved experimental results in the charm threshold region have become available [5], and at the same time the moments have been evaluated up to order α_s^2 [6, 7]. A fresh look at the evaluation of the charm quark mass with the help of sum rules is thus an obvious task. We will concentrate on low moments, say up to the fourth one and present the results for the fifth to the eighth moment just for illustration. This is a natural route to determine directly a short distance mass, say $m_c(m_c)$ or even $m_c(3\text{ GeV})$ in the $\overline{\text{MS}}$ scheme as advocated in the original papers [1, 8]. In the present work we concentrate on the mass in the $\overline{\text{MS}}$ scheme, $m_c(\mu)$, and adopt $\mu = 3$ GeV as our default value, a scale characteristic for the present problem and sufficiently high to ensure convergence of the perturbative series. As already discussed in [1], fixed order pQCD is adequate, if only low moments are used in the analysis.

Recently the determination of the charm quark mass got quite some attention. In [9] the pole mass M_c has been determined from the comparison of the direct determination of the hadronic contribution to $\Delta\alpha(M_Z)$ with the determination using analytical continuation. This leads to the range $M_c = 1.33 - 1.40$ GeV [9]. The pole mass has also been determined in [10] using QCD sum rules in combination with nonrelativistic QCD. Their result reads $M_c = 1.70(13)$ GeV and is significantly higher than the one of Ref. [9]. The

$\overline{\rm MS}$ mass given in [10] reads $m_c(m_c) = 1.23(9)$ GeV. On the basis of so-called Chauchy sum rules, recent experimental data and analytical results for the three-loop photon polarization function the $\overline{\rm MS}$ charm quark mass has been determined in [11] with the result $m_c(m_c) = 1.37(9)$ GeV. In [12] pseudo-scalar sum rules have been used to determine simultaneously the decay constant f_D and the charm quark mass. For the latter the value $m_c(m_c) = 1.10(4)$ GeV is given in the abstract of [12] which is significantly lower than the other evaluations.

We also want to mention that there is a recent lattice evaluation of the charm quark mass [13] with the result $m_c(m_c) = 1.26(4)(12)$ GeV. The first error corresponds to the statistical and the second one to the systematical uncertainty. Note that this result is derived in quenched QCD and the corresponding uncertainty is not included.

In the remaining part of the Introduction we would like to fix the notation and define the quantities we are dealing with in the remainder of the paper.

It is convenient to normalize the radiatively corrected hadronic cross section and to define the ratio

$$R(s) \;=\; \frac{\sigma(e^+e^- \to \text{hadrons})}{\sigma_{\rm pt}}\,, \tag{1}$$

where $\sigma_{\rm pt} = 4\pi\alpha^2/(3s)$. As an inclusive quantity $R(s)$ is conveniently obtained via the optical theorem from the imaginary part of the polarization function of two vector currents via

$$R(s) \;=\; 12\pi\,{\rm Im}\left[\Pi(q^2 = s + i\epsilon)\right]\,, \tag{2}$$

where $\Pi(q^2)$ is defined through

$$\left(-q^2 g_{\mu\nu} + q_\mu q_\nu\right)\,\Pi(q^2) \;=\; i\int {\rm d}x\, e^{iqx}\langle 0|Tj_\mu(x)j_\nu^\dagger(0)|0\rangle\,, \tag{3}$$

with j_μ being the electromagnetic current.

The perturbative expansion of $R(s)$ can be written as

$$R(s) \;=\; \sum_Q R_Q^{(0)} + \frac{\alpha_s}{\pi}R_Q^{(1)} + \left(\frac{\alpha_s}{\pi}\right)^2 R_Q^{(2)} + \left(\frac{\alpha_s}{\pi}\right)^3 R_Q^{(3)} + \ldots\,, \tag{4}$$

where the summation is performed over all active quark flavours Q. (We ignore the small singlet contribution at order α_s^3.) For a comprehensive compilation of the individual pieces we refer to [14, 15] where also explicit results are given. We want to stress that the full quark mass dependence is available up to order α_s^2 [6, 7]. In the case of $R_Q^{(3)}$ the first three terms in the high-energy expansion are known [16].

Our theoretical predictions are based on Eq. (4) where the up, down and strange quark masses are taken to be massless and for the charm and bottom quark the respective pole masses are chosen as input. If not stated otherwise we will use the following input values for the evaluation of $R(s)$

$$\begin{aligned} \alpha_s^{(5)}(M_Z) &= 0.118 \pm 0.003\,, \\ M_c &= (1.65 \pm 0.15)\ \mathrm{GeV}\,, \\ M_b &= (4.75 \pm 0.20)\ \mathrm{GeV}\,, \end{aligned} \tag{5}$$

which cover the full range of all currently accepted results.

At several places of our analysis the renormalization group functions and the matching conditions for the masses and the strong coupling are needed in order to get relations between different energy scales. The corresponding calculations are performed using the package `RunDec` [17].

The outline of the paper is as follows: in Section 2 we compare the experimental data of $R(s)$ with the theoretical prediction and determine α_s from the continuum data below $\sqrt{s} = 3.73$ GeV and above $\sqrt{s} = 4.8$ GeV. The measurement in the charm threshold region is used for the determination of the charm quark mass in Section 3. Similar considerations are used in Section 4 in order to obtain the bottom quark mass. Section 5 contains our conclusions.

2 The continuum region

As stated in the Introduction, we distinguish two energy regions: first, the continuum region where pQCD and local duality are expected to give reliable predictions for the hadronic cross section and, second, the charm threshold region starting from the D meson threshold at 3.73 GeV up to approximately 5 GeV, where the cross section exhibits rapid variations, plus the J/Ψ and Ψ' resonances. The former will be mainly sensitive to the value of α_s. The latter will be used to evaluate moments and to determine the charm quark mass. For the present analysis the continuum region covers the BES data points from 2 GeV up to 3.73 GeV and the data from BES [5], MD-1 [18] and CLEO [19] between 4.8 GeV and 10.52 GeV[1]. As is evident from Fig. 1 pQCD with $\alpha_s^{(5)}(M_Z) = 0.118$ provides an excellent description of all recent results.

Below 3.73 GeV only u, d and s quarks are produced and the $\mathcal{O}(\alpha_s^3)$ approximation for massless quarks is adequate for a description of R. The effective number of flavours is chosen to be $n_f = 3$ and virtual charm quark effects are taken into account (for a compilation of the relevant formulae see Ref. [14, 15]). Above charm threshold u, d and s quark production is calculated as before, however, with $n_f = 4$. Up to $\mathcal{O}(\alpha_s^2)$ the prediction for the charm quark production incorporates the full M_c dependence. Starting from order α_s^2 also the M_c dependence of "secondary" charm production has to be taken into account. This includes diagrams of the type in Fig. 2(a) as well as those from Fig. 2(b). In addition we include $\mathcal{O}(\alpha_s^3)$ terms from the expansion in $(M_c^2/s)^n$ with $n = 0, 1$

[1]We limit this analysis to more recent results from BES [5], those from MD-1 [18] and from CLEO [19] with systematic errors of typically 4.3%, 4% and 2%, respectively. Older measurements, in particular those from SPEAR and DORIS, are consistent with the new results. However, with their significantly larger errors they do not provide additional information.

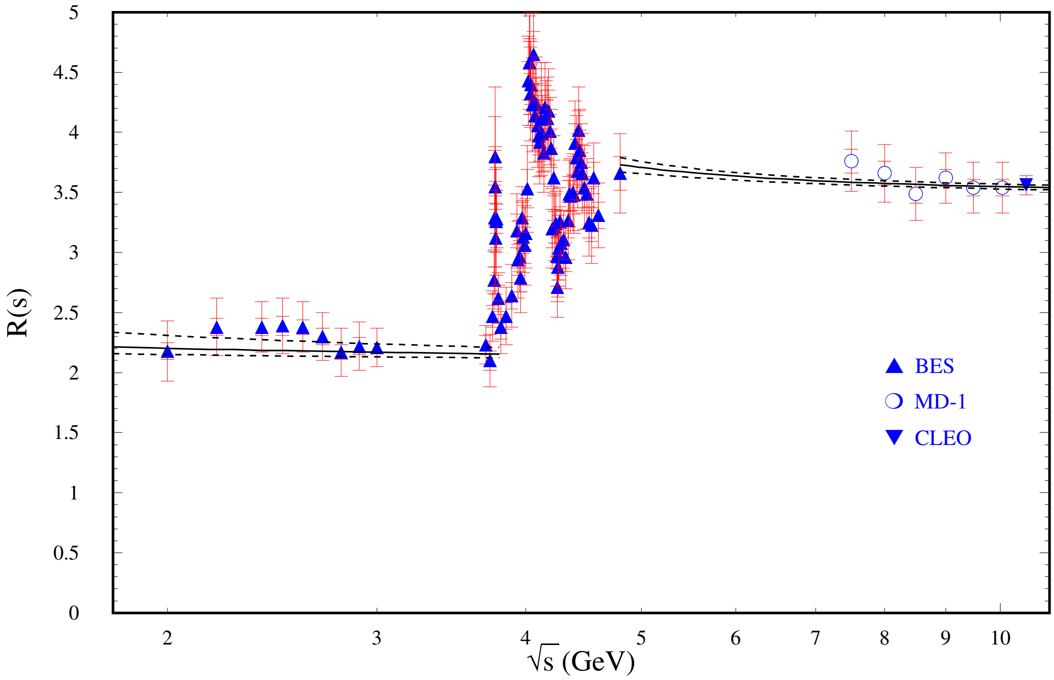

Figure 1: $R(s)$ in the energy range between 1.8 GeV and 11.0 GeV. The solid line corresponds to the theoretical predictions adopting our central values for the input parameters. The theoretical uncertainties are indicated by the dashed curves which are obtained from the variation of the input parameters as described in the text. The two error bars on the data points indicate the statistical (inner) and systematical (outer) uncertainty.

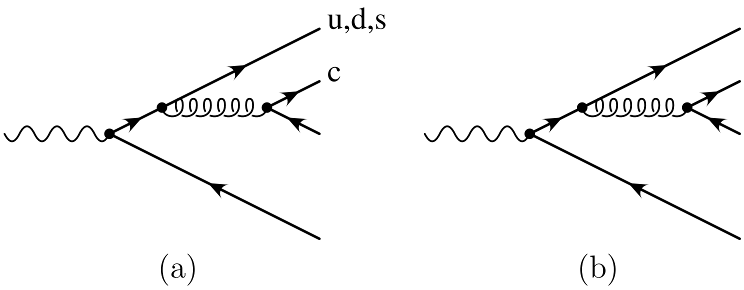

Figure 2: Feynman diagrams contributing to $R(s)$ at order α_s^2. A secondary charm quark pair is produced through gluon splitting.

and 2 [14, 16]. Last not least contributions from virtual c quarks ($\sqrt{s} \leq 3.73$ GeV) and b quarks ($\sqrt{s} \leq 10.52$ GeV) have been calculated which are suppressed $\sim (\alpha_s/\pi)^2 s/(4M^2)$ and decouple for $s \ll 4M^2$. These are included in the fifth column of Tab. 1. Pure QED final state radiation is tiny and taken into account for completeness. (For a related analysis at $\sqrt{s} = 10.5$ GeV see [20].)

The magnitude of the most important terms is shown for several characteristic energies in Tab. 1 and compared to the experimental results. All numbers are given for the

$\sqrt{s}$ (GeV)	n_f	$\alpha_s^{(n_f)}(\sqrt{s})$	u, d, s	c, b	$R^{\rm th}(s)$	$R^{\rm exp}(s)$
2.000	3	0.297	2.202	0.002	2.203	2.180± 0.070
3.730	3	0.226	2.154	0.002	2.156	2.100± 0.080
4.800	4	0.215	2.146	1.607	3.753	3.660± 0.140
8.900	4	0.180	2.122	1.440	3.562	3.579± 0.066
10.520	4	0.172	2.117	1.427	3.544	3.560± 0.010

Table 1: In the last two columns the experimental values for $R(s)$ are compared with the theoretical prediction, $R^{\rm th}(s)$, for a selected number of energies where $\mu^2 = s$ has been adopted (see text). For completeness we list the number of active flavours, n_f, and the values of $\alpha_s^{(n_f)}(\sqrt{s})$.

reference values as specified in Eq. (5). The band in Fig. 1 is obtained from the corresponding errors and the theoretical uncertainty from the variation of the renormalization scale between $\mu^2 = s/4$ and $\mu^2 = 4s$ which have been added quadratically. The excellent agreement between prediction and measurement suggests that one might determine α_s from this analysis.

Assigning a fully correlated systematic error of 4.3% to the BES data [21] we find

$$\alpha_s^{(3)}(3\ \text{GeV}) \quad = \quad 0.369^{+0.047+0.123}_{-0.046-0.130}\,, \tag{6}$$

from the BES data below 3.73 GeV and

$$\alpha_s^{(4)}(4.8\ \text{GeV}) \quad = \quad 0.183^{+0.059+0.053}_{-0.064-0.057}\,, \tag{7}$$

from the point at 4.8 GeV. The uncertainties refer to the uncorrelated (statistical) and correlated errors, respectively. The same analysis is applicable to the MD-1 results. On the basis of the R values listed for six energies in their table 4 and assuming fully correlated systematic errors we find

$$\alpha_s^{(4)}(8.9\ \text{GeV}) \quad = \quad 0.201^{+0.026+0.129}_{-0.025-0.109}\,. \tag{8}$$

From their average value $R((8.9\ \text{GeV})^2) = 3.578{\pm}0.021{\pm}0.140$ as quoted in their summary we obtain[2]

$$\alpha_s^{(4)}(8.9\ \text{GeV}) \quad = \quad 0.193^{+0.017+0.127}_{-0.017-0.107}\,, \tag{9}$$

consistent with Eq. (8) but with smaller errors. From the CLEO value $R((10.52\ \text{GeV})^2) = 3.56 \pm 0.01 \pm 0.07$ we deduce

$$\alpha_s^{(4)}(10.52\ \text{GeV}) \quad = \quad 0.186^{+0.008+0.061}_{-0.008-0.057}\,. \tag{10}$$

[2]This result disagrees from their value $\alpha_s^{(4)}(8.9\ \text{GeV}) = 0.174 \pm 0.039$ as a consequence of their inadequate treatment of the quark mass effects.

We combine the results of Eqs. (6), (7), (9) and (10) by assuming uncorrelated systematic errors and evolving them to a common scale of 5 GeV. Combining the errors in quadrature we find

$$\alpha_s^{(4)}(5\text{ GeV}) \;=\; 0.235^{+0.047}_{-0.047}\,. \tag{11}$$

Evolving this value up to M_Z

$$\alpha_s^{(5)}(M_Z) \;=\; 0.124^{+0.011}_{-0.014}\,, \tag{12}$$

good agreement with other determinations [22, 23] is observed.

3 Charm quark mass determination from the threshold region

The first method we want to use for the determination of the charm quark mass is based on the direct comparison of theoretical and experimental moments of the charm quark contribution to the photon polarization function as defined in Eq. (3). In the limit of small momentum the latter can be cast into the form [7]

$$\Pi_c(q^2) \;=\; Q_c^2 \frac{3}{16\pi^2} \sum_{n\geq 0} \bar{C}_n z^n\,, \tag{13}$$

with $Q_c = 2/3$ and $z = q^2/(4m_c^2)$ where $m_c = m_c(\mu)$ is the $\overline{\mathrm{MS}}$ charm quark mass at the scale μ. The perturbative series for the coefficients $\bar{C}_n$ up to $n = 8$ is known analytically [6, 7] up to order α_s^2. The coefficients also depend on the charm quark mass through logarithms of the form $l_{m_c} \equiv \ln(m_c^2(\mu)/\mu^2)$ and can be written as

$$\bar{C}_n \;=\; \bar{C}_n^{(0)} + \frac{\alpha_s(\mu)}{\pi}\left(\bar{C}_n^{(10)} + \bar{C}_n^{(11)} l_{m_c}\right) + \left(\frac{\alpha_s(\mu)}{\pi}\right)^2 \left(\bar{C}_n^{(20)} + \bar{C}_n^{(21)} l_{m_c} + \bar{C}_n^{(22)} l_{m_c}^2\right)\,. \tag{14}$$

In Tab. 2 the individual coefficients are given in numerical form. They essentially constitute our theoretical input. We define the moments

$$\mathcal{M}_n \;\equiv\; \frac{12\pi^2}{n!}\left(\frac{\mathrm{d}}{\mathrm{d}q^2}\right)^n \Pi_c(q^2)\bigg|_{q^2=0}\,, \tag{15}$$

which leads to

$$\mathcal{M}_n^{\mathrm{th}} \;=\; \frac{9}{4} Q_c^2 \left(\frac{1}{4m_c^2}\right)^n \bar{C}_n\,. \tag{16}$$

n	1	2	3	4	5	6	7	8
$\bar{C}_n^{(0)}$	1.0667	0.4571	0.2709	0.1847	0.1364	0.1061	0.0856	0.0709
$\bar{C}_n^{(10)}$	2.5547	1.1096	0.5194	0.2031	0.0106	−0.1158	−0.2033	−0.2660
$\bar{C}_n^{(11)}$	2.1333	1.8286	1.6254	1.4776	1.3640	1.2730	1.1982	1.1351
$\bar{C}_n^{(20)}$	2.4967	2.7770	1.6388	0.7956	0.2781	0.0070	−0.0860	−0.0496
$\bar{C}_n^{(21)}$	3.3130	5.1489	4.7207	3.6440	2.3385	0.9553	−0.4423	−1.8261
$\bar{C}_n^{(22)}$	−0.0889	1.7524	3.1831	4.3713	5.3990	6.3121	7.1390	7.8984

Table 2: Coefficients of the photon polarization function in the $\overline{\rm MS}$ scheme as defined in Eqs. (13) and (14). $n_f = 4$ has been adopted which is appropriate for the charm threshold.

With the help of a dispersion relation we establish the connection between the polarization function and the experimentally accessible cross section $R_c(s)$. In the $\overline{\rm MS}$ scheme

$$\Pi_c(q^2) = \frac{q^2}{12\pi^2}\int {\rm d}s\,\frac{R_c(s)}{s(s-q^2)} + Q_c^2\frac{3}{16\pi^2}\bar{C}_0\,, \tag{17}$$

which allows to determine the experimental moments

$$\mathcal{M}_n^{\rm exp} = \int \frac{{\rm d}s}{s^{n+1}}R_c(s)\,. \tag{18}$$

Note, that the last term in Eq. (17) which defines the renormalization scheme disappears after taking derivatives with respect to q^2. Equating Eqs. (16) and (18) leads to an expression from which the charm quark mass can be obtained:

$$m_c(\mu) = \frac{1}{2}\left(\frac{\bar{C}_n}{\mathcal{M}_n^{\rm exp}}\right)^{1/(2n)}\,. \tag{19}$$

As a second method we consider the ratio of two successive moments which leads to

$$m_c(\mu) = \frac{1}{2}\sqrt{\frac{\mathcal{M}_n^{\rm exp}}{\mathcal{M}_{n+1}^{\rm exp}}\frac{\bar{C}_{n+1}}{\bar{C}_n}}\,. \tag{20}$$

Here the normalization uncertainty of the experimental data is largely cancelled. Both in Eqs. (19) and (20) one has to remember the m_c dependence of $\bar{C}_n$.

We have checked that the nonperturbative contribution from gluon condensates [1, 24] can be neglected within the present accuracy.

Let us now turn to the extraction of the experimental values for the three different contributions which enter the right-hand side of Eq. (18): the J/Ψ and Ψ' resonances ($\mathcal{M}_n^{\rm exp,res}$), the charm threshold region between $2M_{D_0} \approx 3.73$ GeV and $\sqrt{s_1} = 4.8$ GeV as measured by the BES experiment [5] ($\mathcal{M}_n^{\rm exp,cc}$), and the continuum contribution above s_1 ($\mathcal{M}_n^{\rm cont}$).

The resonances are treated in the narrow width approximation which corresponds to

$$R^{\rm res}(s) \;=\; \frac{9\pi M_R\Gamma_e}{\alpha^2}\left(\frac{\alpha}{\alpha(s)}\right)^2 \delta(s-M_R^2)\,, \tag{21}$$

with $\alpha^{-1} = 137.0359895$. For both resonances we use $(\alpha/\alpha(s))^2 \approx 0.9562$ and $M_{J/\Psi} = 3.09687(4)$ MeV, $\Gamma_e^{J/\Psi} = 5.26(37)$ keV, $M_{\Psi'} = 3.68596(9)$ MeV and $\Gamma_e^{\Psi'} = 2.12(18)$ keV [22].

In the charm threshold region we have to identify the contribution from the charm quark, i.e. we have to subtract the parts arising from the light u, d and s quark from the data. Technically this is done by determining a mean value for $R_{uds} \equiv R_u + R_d + R_s$ from the comparison of theoretical predictions and the BES data between 2 GeV and 3.73 GeV and using the theoretically predicted energy dependence to extrapolate into the region between 3.73 GeV and 4.8 GeV [25]. This value is subtracted from the data before the integration is performed. Alternatively, one could adopt the massless prediction for $R(s)$ up to order α_s^3 without taking into account the data below $\sqrt{s} = 3.73$ GeV. We checked that both approaches lead to the same final result.

In the continuum region above $\sqrt{s} = 4.8$ GeV there is only sparse and quite unprecise data. On the other hand pQCD provides reliable predictions for $R(s)$, which is essentially due to the knowledge of the complete mass dependence up to order α_s^2 [6]. Thus in this region we will replace data by the theoretical prediction for $R(s)$ as discussed in Section 2.

In Tab. 3 we present the results for the moments separated according to the three different contributions discussed above. The error of the resonance contribution is due to the uncertainties of the input parameters. In the case of the charm threshold contribution the uncertainty is dominated by the correlated normalization error of approximately 4.3% of the BES data. In the continuum region we varied the input parameters as as stated in Eq. (5) and the renormalization scale as $\mu = (3 \pm 1)$ GeV. The errors of the three contributions are added quadratically. It is illustrating to compare the composition of the experimental error for the different moments. Generally speaking, it is dominated by the resonance contribution, specifically by the 7% and 9% uncertainty in the leptonic widths of the J/Ψ and Ψ', respectively. For the moment with $n = 1$ and to some extent the one with $n = 2$ the improvement in the cross section measurement due to BES (from about $10 - 20$ % systematic error down to 4.3%) was important. The parametric uncertainties (from α_s and M_c) and the residual μ-dependence which affect $\mathcal{M}_n^{\rm cont}$ are small. The higher moments (in fact already for n above two) are increasingly dominated by the resonance contributions with their 7% uncertainty.

We use the results of Tab. 3 together with Eq. (19) in order to obtain in a first step $m_c(3\,\text{GeV})$. Subsequently the result is transformed to the scale-invariant mass $m_c(m_c)$ [17] including the three-loop coefficients of the renormalization group functions. Both results can be found in Tab. 4. The starting value for $\alpha_s(3\,\text{GeV}) = 0.254^{+0.015}_{-0.014}$ needed for this step is obtained from $\alpha_s(M_Z) = 0.118 \pm 0.003$ by using the renormalization group equations and the matching conditions with four loop accuracy.

The errors listed in Tab. 4 receive contributions from the uncertainties in the experimental moments and the variation of α_s (cf. Eq. (5)) and $\mu = (3 \pm 1)$ GeV in the

n	$\mathcal{M}_n^{\rm exp,res}$ $\times 10^{(n-1)}$	$\mathcal{M}_n^{\rm exp,cc}$ $\times 10^{(n-1)}$	$\mathcal{M}_n^{\rm cont}$ $\times 10^{(n-1)}$	$\mathcal{M}_n^{\rm exp}$ $\times 10^{(n-1)}$
1	0.1114(82)	0.0313(15)	0.0638(10)	0.2065(84)
2	0.1096(79)	0.0174(8)	0.0142(3)	0.1412(80)
3	0.1094(79)	0.0099(5)	0.0042(1)	0.1234(79)
4	0.1105(79)	0.0057(3)	0.0014(0)	0.1175(79)
5	0.1126(80)	0.0033(2)	0.0005(0)	0.1164(80)
6	0.1155(82)	0.0020(1)	0.0002(0)	0.1176(82)
7	0.1190(84)	0.0012(1)	0.0001(0)	0.1202(84)
8	0.1230(87)	0.0007(0)	0.0000(0)	0.1237(87)

Table 3: Experimental moments as defined in Eq. (18) separated according to the contributions from the resonances, the charm threshold region and the continuum region above $\sqrt{s} = 4.8$ GeV.

n	1	2	3	4
m_c(3 GeV)	1.027(30)	0.994(37)	0.961(59)	0.997(67)
$m_c(m_c)$	1.304(27)	1.274(34)	1.244(54)	1.277(62)
n	5	6	7	8
m_c(3 GeV)	1.094(110)	1.184(161)	1.253(182)	1.307(191)
$m_c(m_c)$	1.366(100)	1.447(146)	1.510(165)	1.558(172)

Table 4: Results for m_c(3 GeV) and $m_c(m_c)$ in GeV obtained from Eq. (19).

coefficients $\bar{C}_n$ which are all added quadratically. It is interesting to note that the uncertainty in m_c(3 GeV) induced by the experimental moments decreases from 0.028 for $n = 1$ to 0.010 for $n = 4$ whereas the theoretical uncertainty from the renormalization scale increases from 0.001 to 0.064, the one from α_s from 0.011 to 0.019.

The moment with $n = 1$ is evidently least sensitive to nonperturbative contributions from condensates, to the Coulombic higher order effects, the variation of μ and the parametric α_s dependence. Hence we adopt

$$m_c(m_c) \;=\; 1.304(27)\ \text{GeV}\,. \tag{22}$$

as our final result. Using the two- and three-loop relation [26, 27, 28] between the pole- and the $\overline{\rm MS}$-mass this corresponds to

$$\begin{aligned} M_c^{(2-\text{loop})} &= 1.514(34)\ \text{GeV}\,, \\ M_c^{(3-\text{loop})} &= 1.691(35)\ \text{GeV}\,. \end{aligned} \tag{23}$$

Our result agrees within the uncertainties with the recent determinations of $m_c(m_c)$ in [10, 11] but is comparatively more precise.

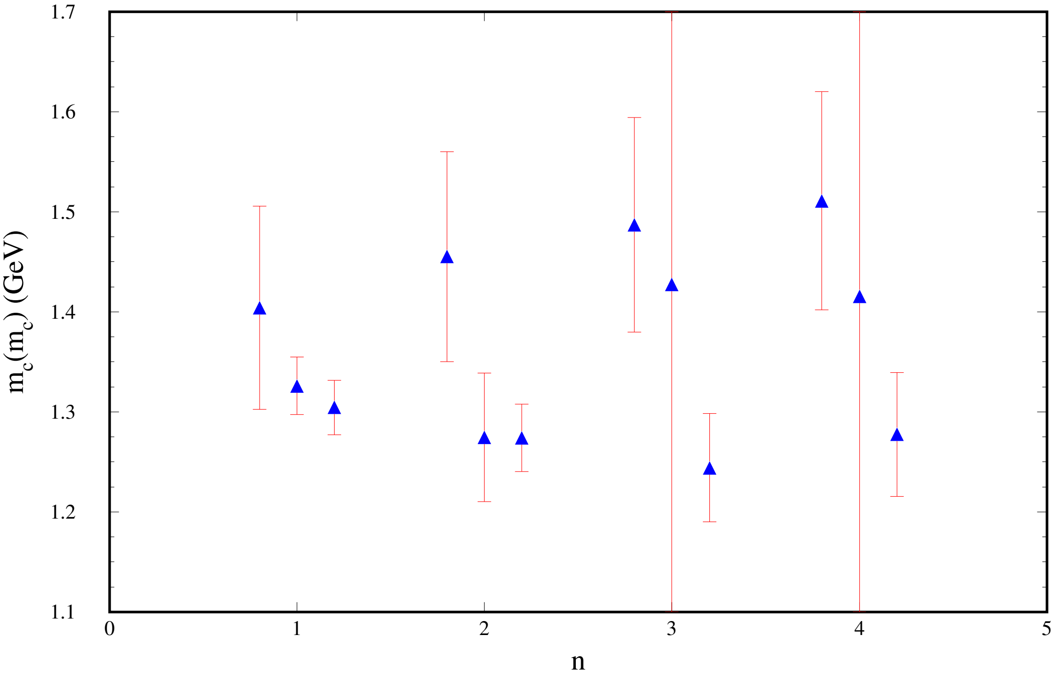

Figure 3: $m_c(m_c)$ for $n = 1, 2, 3$ and 4. For each value of n the results from left to right correspond the inclusion of terms of order α_s^0, α_s^1 and α_s^2 in the coefficients $\bar{C}_n$ (cf. Eq. (14)). Note, that for $n = 3$ and $n = 4$ the errors can not be determined with the help of Eq. (19) in those cases where only the two-loop corrections of order α_s are included into the coefficients $\bar{C}_n$ as the equation cannot be solved for $m_c(3\ \text{GeV})$.

In Fig. 3 we compare the results for $m_c(m_c)$ (and its μ dependence) based on the theory moments ($n = 1, \ldots, 4$) evaluated up to $\mathcal{O}(\alpha_s^0)$, $\mathcal{O}(\alpha_s^1)$ and $\mathcal{O}(\alpha_s^2)$, respectively. The improved stability with increasing order in α_s is evident, and the preference for the first moment is clearly visible.

As an alternative we also present the mass values derived from the ratio of moments (Eq. (20)) in Tab. 5. The error is obtained from the quadratic combination of the uncertainties induced by the resonances, the integration in the charm threshold region, the continuum contribution and the independent variation of α_s and μ in the coefficients $\bar{C}_n$. It is significantly larger than the one based on the analysis of the moments. The numbers are therefore compatible with Eq. (22) but do not improve upon this result.

4 The bottom quark mass

The same approach is also applicable to the determination of m_b. The coefficients $\bar{C}_n$ are listed in Tab. 6. They determine the theoretical moments through Eq. (16) where Q_c has to be replaced by $Q_b = -1/3$. The experimental results for the moments are listed in Tab. 7. The contribution from the resonances include $\Upsilon(1S)$ up to $\Upsilon(6S)$ and are given by $\mathcal{M}_n^{\text{exp,res}}$. The treatment of the region between $\sqrt{s} = 11.075$ GeV and $\sqrt{s} = 11.2$ GeV

$n/(n+1)$	1/2	2/3	3/4	4/5
$m_c(3\ \text{GeV})$	0.954(64)	0.876(340)	1.052(153)	1.259(261)
$m_c(m_c)$	1.238(59)	1.166(318)	1.327(140)	1.515(236)
$n/(n+1)$	5/6	6/7	7/8	
$m_c(3\ \text{GeV})$	1.434(339)	1.574(386)	1.679(408)	
$m_c(m_c)$	1.671(304)	1.795(344)	1.886(361)	

Table 5: Results for $m_c(3\ \text{GeV})$ and $m_c(m_c)$ in GeV obtained from Eq. (20).

n	1	2	3	4	5	6	7	8
$\bar{C}_n^{(0)}$	1.0667	0.4571	0.2709	0.1847	0.1364	0.1061	0.0856	0.0709
$\bar{C}_n^{(10)}$	2.5547	1.1096	0.5194	0.2031	0.0106	−0.1158	−0.2033	−0.2660
$\bar{C}_n^{(11)}$	2.1333	1.8286	1.6254	1.4776	1.3640	1.2730	1.1982	1.1351
$\bar{C}_n^{(20)}$	3.1590	3.2319	2.0677	1.2204	0.7023	0.4304	0.3359	0.3701
$\bar{C}_n^{(21)}$	3.4425	5.0798	4.5815	3.4726	2.1508	0.7592	−0.6426	−2.0281
$\bar{C}_n^{(22)}$	0.0889	1.9048	3.3185	4.4945	5.5127	6.4182	7.2388	7.9929

Table 6: Coefficients of the photon polarization function in the $\overline{\text{MS}}$ scheme as defined in Eqs. (13) and (14). $n_f = 5$ has been adopted which is appropriate for the bottom threshold.

follows [25]. We assume a linear raise from zero to the pQCD prediction $R_b((11.2\ \text{GeV})^2)$ and the take the contribution itself as an estimate for the error. Note that the contribution to the moments, $\mathcal{M}_n^{\text{exp,lin}}$ is negligible small. Above 11.2 GeV we use the prediction from pQCD for $R_b(s)$ which results in the moments $\mathcal{M}_n^{\text{cont}}$.

The uncertainties are completely analogous to the charm quark case. The only difference concerns the renormalization scale for which we adopt $\mu = (10 \pm 5)$ GeV.

The results for $m_b(10\ \text{GeV})$ and $m_b(m_b)$ are listed in Tab. 8. A remarkable consistency and stability is observed. For $n = 1$ the error is dominated by the experimental input. For $n = 3$ we obtain ± 0.036 from the experimental input, ± 0.025 from α_s and ± 0.020 from the variation of μ.

The sensitivity to the inclusion of higher orders is displayed in Fig. 4. Again a significant improvement of the stability of our prediction is observed. As our final result we adopt

$$m_b(m_b) = 4.191(51)\ \text{GeV}\,, \tag{24}$$

well consistent with evaluations based on the analysis of bottonium and high spectral moments [29, 30, 31, 32, 33] (see also [22])[3]. The $\overline{\text{MS}}$ result of Eq. (24) corresponds to a

[3]Our result also agrees with the one of Ref. [34]. However, in [34] the bottom quark mass has been determined from relatively large moments ($7 \leq n \leq 15$), a highly disputable treatment of the threshold has been employed and no stability for small n has been observed.

n	$\mathcal{M}_n^{\rm exp,res}$ $\times 10^{(2n+1)}$	$\mathcal{M}_n^{\rm exp,lin}$ $\times 10^{(2n+1)}$	$\mathcal{M}_n^{\rm cont}$ $\times 10^{(2n+1)}$	$\mathcal{M}_n^{\rm exp}$ $\times 10^{(2n+1)}$
1	1.508(114)	0.035(35)	2.913(21)	4.456(121)
2	1.546(109)	0.028(28)	1.182(12)	2.756(113)
3	1.600(106)	0.022(22)	0.634(8)	2.256(108)
4	1.671(104)	0.018(18)	0.381(5)	2.070(105)
5	1.761(103)	0.014(14)	0.244(3)	2.019(104)
6	1.870(104)	0.012(12)	0.162(2)	2.044(104)
7	1.998(105)	0.009(9)	0.111(2)	2.119(106)
8	2.149(108)	0.007(7)	0.078(1)	2.234(109)

Table 7: Moments for the bottom quark system.

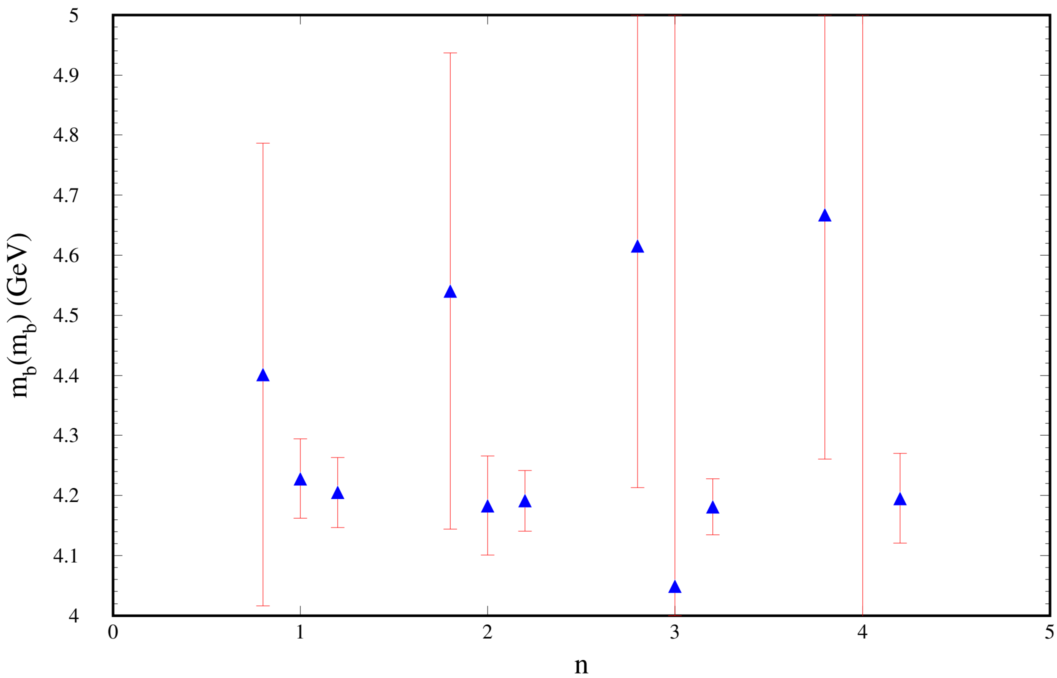

Figure 4: $m_b(m_b)$ for $n = 1, 2, 3$ and 4. For each value of n the results from left to right correspond the inclusion of terms of order α_s^0, α_s^1 and α_s^2 in the coefficients $\bar{C}_n$ (cf. Eq. (14)). Note, that the errors for $n = 3$ and both the central value and the errors for $n = 4$ can not be determined in those cases where only the two-loop corrections of order α_s are included into the coefficients $\bar{C}_n$ as the corresponding equation cannot be solved for $m_b(10 \text{ GeV})$.

pole mass of [26, 27, 28]

$$
\begin{aligned}
M_b^{(2-\rm loop)} &= 4.651(57)\ \text{GeV}\,,\\
M_b^{(3-\rm loop)} &= 4.819(57)\ \text{GeV}\,,
\end{aligned}
\tag{25}
$$

n	1	2	3	4
m_b(10 GeV)	3.665(60)	3.651(52)	3.641(48)	3.655(77)
$m_b(m_b)$	4.205(58)	4.191(51)	4.181(47)	4.195(75)
n	5	6	7	8
m_b(10 GeV)	3.720(195)	3.833(293)	3.965(347)	4.089(436)
$m_b(m_b)$	4.258(189)	4.367(285)	4.494(335)	4.614(420)

Table 8: Results for m_b(10 GeV) and $m_b(m_b)$ in GeV obtained from Eq. (19) as described in the text.

$n/(n+1)$	1/2	2/3	3/4	4/5
m_b(10 GeV)	3.636(52)	3.620(51)	3.694(240)	3.915(523)
$m_b(m_b)$	4.177(51)	4.161(50)	4.233(233)	4.446(507)
$n/(n+1)$	5/6	6/7	7/8	
m_b(10 GeV)	4.218(717)	4.523(875)	4.786(1.113)	
$m_b(m_b)$	4.737(692)	5.028(839)	5.277(1.063)	

Table 9: Results for m_b(10 GeV) and $m_b(m_b)$ in GeV obtained from Eq. (20) as described in the text.

using $\mathcal{O}(\alpha_s^2)$ and $\mathcal{O}(\alpha_s^3)$ accuracy, respectively.

5 Conclusions

Recent experimental data for the total cross section $\sigma(e^+e^- \to \text{hadrons})$ have been compared with the up-to-date theoretical prediction of perturbative QCD for those energies where perturbation theory is reliable. The excellent agreement justifies the determination of the strong coupling α_s from the measurements in the energy region between 2 and 3.73 GeV below the charm threshold and the region between 4.8 and 10.52 GeV above charm and below the bottom threshold. Our result $\alpha_s(5\text{ GeV}) = 0.235^{+0.047}_{-0.047}$ corresponds to $\alpha_s(M_Z) = 0.124^{+0.011}_{-0.014}$ and serves as a useful cross check in the intermediate energy region but is less precise than those from τ- or Z-boson decays.

The direct determination of the short distance $\overline{\text{MS}}$ charm quark mass is performed with the help of the precise data from the charm threshold region and the three loop evaluation of moments in pQCD. Using low moments the approach is insensitive to the Coulombic behaviour of the cross section close to threshold and to nonperturbative condensates. The results based on different moments are quite consistent and the moment with $n = 1$ exhibits the least sensitivity towards the parametric dependence on α_s and the renormalization scale. As our final result we obtain $m_c(m_c) = 1.304(27)$ GeV. The same approach when applied to the bottom quark gives $m_b(m_b) = 4.191(51)$ GeV. These values are compatable with but more precise than other recent analyses.

Acknowledgments

We would like to thank A.A. Penin for carefully reading the manuscript. We thank G. Corcella for drawing our attention to an error in the running from $m_b(10\text{ GeV})$ to $m_b(m_b)$. This work was supported in part by the *DFG-Forschergruppe "Quantenfeldtheorie, Computeralgebra und Monte-Carlo-Simulation"* (contract FOR 264/2-1) and by SUN Microsystems through Academic Equipment Grant No. 14WU0148.

References

[1] V. A. Novikov *et al.*, Phys. Rep. C **41** (1978) 1.

[2] for a review see: L. J. Reinders, H. Rubinstein, and S. Yazaki, Phys. Rept. **127** (1985) 1.

[3] M. Beneke, Phys. Lett. B **434** (1998) 115.

[4] A. H. Hoang, M. C. Smith, T. Stelzer, and S. Willenbrock, Phys. Rev. D **59** (1999) 114014.

[5] J. Z. Bai *et al.*, hep-ex/0102003.

[6] K. G. Chetyrkin, J. H. Kühn, and M. Steinhauser, Phys. Lett. B **371** (1996) 93; Nucl. Phys. B **482** (1996) 213.

[7] K. G. Chetyrkin, J. H. Kühn, and M. Steinhauser, Nucl. Phys. B **505** (1997) 40.

[8] M. A. Shifman, A. I. Vainshtein, and V. I. Zakharov, Nucl. Phys. B **147** (1979) 385; Nucl. Phys. B **147** (1979) 448.

[9] A. D. Martin, J. Outhwaite, and M. G. Ryskin, Eur. Phys. J. C **19** (2001) 681.

[10] M. Eidemüller and M. Jamin, Phys. Lett. B **498** (2001) 203.

[11] J. Penarrocha and K. Schilcher, Phys. Lett. B **515** (2001) 291.

[12] S. Narison, hep-ph/0108242.

[13] D. Becirevic, V. Lubicz, and G. Martinelli, hep-ph/0107124.

[14] K. G. Chetyrkin, J. H. Kühn, and A. Kwiatkowski, Phys. Reports **277** (1997) 189.

[15] K. G. Chetyrkin, A. H. Hoang, J. H. Kühn, M. Steinhauser, and T. Teubner, Eur. Phys. J. C **2** (1998) 137.

[16] K. G. Chetyrkin, R. V. Harlander, and J. H. Kühn, Nucl. Phys. B **586** (2000) 56.

[17] K. G. Chetyrkin, J. H. Kühn, and M. Steinhauser, Comput. Phys. Commun. **133** (2000) 43.

[18] A. E. Blinov *et al.*, Z. Phys. C **70** (1996) 31.

[19] R. Ammar *et al.*, Phys. Rev. D **57** (1998) 1350.

[20] K. G. Chetyrkin and J. H. Kühn, Phys. Lett. B **342** (1995) 356;
K. G. Chetyrkin, J. H. Kühn, and T. Teubner, Phys. Rev. D **56** (1997) 3011.

[21] Z. G. Zhao, private communication.

[22] D. E. Groom et al., Eur. Phys. J. C **15** (2000) 1.

[23] B. A. Kniehl, G. Kramer, and B. Pötter, Phys. Rev. Lett. **85** (2000) 5288.

[24] D. J. Broadhurst, P. A. Baikov, V. A. Ilin, J. Fleischer, O. V. Tarasov and V. A. Smirnov, Phys. Lett. B **329** (1994) 103.

[25] J. H. Kühn and M. Steinhauser, Phys. Lett. B **437** (1998) 425.

[26] N. Gray, D. J. Broadhurst, W. Grafe, and K. Schilcher, Z. Phys. C **48** (1990) 673.

[27] K. G. Chetyrkin and M. Steinhauser, Phys. Rev. Lett. **83** (1999) 4001;
K. G. Chetyrkin and M. Steinhauser, Nucl. Phys. B **573** (2000) 617.

[28] K. Melnikov and T. v. Ritbergen, Phys. Lett. B **482** (2000) 99.

[29] J. H. Kühn, A. A. Penin, and A. A. Pivovarov, Nucl. Phys. B **534**, 356 (1998);
A. A. Penin and A. A. Pivovarov, Phys. Lett. B **435** (1998) 413; Nucl. Phys. B **549** (1999) 217.

[30] K. Melnikov and A. Yelkhovsky, Phys. Rev. D **59** (1999) 114009.

[31] M. Beneke and A. Signer, Phys. Lett. B **471** (1999) 233.

[32] A. H. Hoang, hep-ph/0008102.

[33] A. Pineda, JHEP **0106** (2001) 022.

[34] M. Jamin and A. Pich, Nucl. Phys. B **507** (1997) 334.